Analytical Methods

Accepted Manuscript

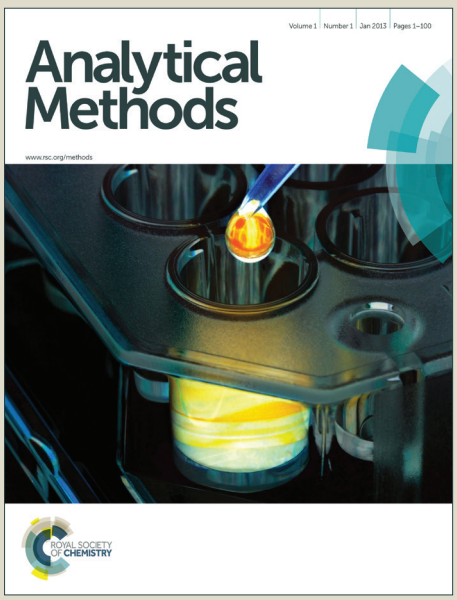

This is an *Accepted Manuscript*, which has been through the Royal Society of Chemistry peer review process and has been accepted for publication.

Accepted Manuscripts are published online shortly after acceptance, before technical editing, formatting and proof reading. Using this free service, authors can make their results available to the community, in citable form, before we publish the edited article. We will replace this *Accepted Manuscript* with the edited and formatted *Advance Article* as soon as it is available.

You can find more information about *Accepted Manuscripts* in the Information for Authors.

ROYAL SOCIETY OF CHEMISTRY

www.rsc.org/methods

Electrochemical detection of 8-hydroxy-2'-deoxyguanosine as a biomarker for oxidative DNA damage in HEK293 cells exposed to 3-chloro-1,2-propanediol

Xiulan Sun[1]*, Lijuan Zhang[1], Hongxia Zhang[2], He Qian[1], Jian Ji[1], Lili Tang[1], Zaijun Li[1], Genyi Zhang[1]*

1 State Key Laboratory of Food Science and Technology, School of Food Science of Jiangnan University, Synergetic Innovation Center of Food Safety and Nutrition, Wuxi, Jiangsu 214122, China

2 School of Foreign Studies, Shanxi University of Technology, Hanzhong, Shanxi 723000, China

***Corresponding author.**

Xiulan Sun*: Tel: +86 510-85329015 ; Fax: +86 510-85328726.

E-mail: sxlzzz@jiangnan.edu.cn

Genyi Zhang*: Tel: +86 510-85329015 ; Fax: +86 510-85328726.

E-mail: genyiz@gmail.com

Abstract:

We investigate here the selective cytotoxicity of 3-Chloro-1,2-propanediol (3-MCPD) on HEK293 cells by analyzing the cell growth inhibition, morphological changes, intracellular reactive oxygen species (ROS) production, and DNA damage. We further demonstrate that 3-MCPD inhibits growth of cells and induces 8-Hydroxy-2'-deoxyguanosine (8-OH-dG) generation via ROS-mediated oxidative DNA damage in HEK293 cells. To provide a detection system, we fabricated a modified electrode with poly(3-acetylthiophene) (P3AT), for electrochemical detection of 8-OH-dG in oxidation-damaged cells. Using electropolymerization cyclic voltammetry (CV), we deposited 3-acetylthiophene (3-AT) on a glassy carbon electrode (GCE). The conducting polymer, P3AT, greatly enhances the peak current via dramatic electrocatalytic effect on the oxidation of 8-OH-dG. We further examined the effects of pre-concentration potential, time, scan rate, and pH value on voltammetric behavior and detection of 8-OH-dG. Under optimal conditions, the anodic peak currents of differential pulse voltammetry (DPV) maintain a linear relationship with 8-OH-dG concentration between 0.5-35 μM, with a correlative coefficient of 0.9963. We estimate the detection limit of 8-OH-dG to be 31.3 nM (S/N = 3). This proposed modified electrode demonstrates excellent reproducibility and stability, making it an ideal candidate for amperometric detection of 8-OH-dG. We performed detection on real cell samples with satisfactory results.

Keywords: 3-Chloro-1,2-propanediol; HEK293 cells; Oxidative DNA damage; 8-Hydroxy-2'-deoxyguanosine; Poly(3-acetylthiophene); Modified glassy carbon electrode

1. Introduction

3-Chloro-1,2-propandiol (3-MCPD) belongs to the chloropropanol class, formed by reaction between hydrochloric acid and residual vegetable fat in the process of producing acid hydrolyzed vegetable protein (HVP). [1] The Joint FAO/WHO Expert Committee on Food Additives (JECFA) has reviewed 3-MCPD toxicity. [2] Studies on the toxicity of 3-MCPD include neurotoxicity, [3] nephrotoxicity, [4] genotoxicity, [5] immunotoxicity, [6] and reproductive toxicity. 3-MCPD has been demonstrated to induce oxidative DNA damage in HEK293 cells. 8-OH-dG is considered a typical biomarker for oxidative DNA damage, [7-9] induced by hydroxy-free radical attack on the guanine residues of DNA, [10, 11] and the most abundant among oxidative DNA products. [12] Therefore, analyses of 8-OH-dG from biological systems *in vitro* and *in vivo* are useful in assessing exposure to various carcinogens, and thus, an individual's cancer risk.

Research on 8-OH-dG detection has yielded several analytical methods including: high-performance liquid chromatography with electrochemical detection (HPLC-ECD), [13-16] capillary electrophoresis with electrochemical detection (CE-ECD), [17, 18] liquid chromatography-coupled mass spectrometry (LC-MS), [19] liquid chromatography combined with electrospray ionization tandem mass spectrometry (LC-MS/MS), [20] gas chromatography-coupled mass spectrometry (GC-MS), [21] and enzyme-linked immuno-absorbent assay (ELISA). [22] However, these methods require complex sample pretreatment as well as pre-concentration with gradient elution during chromatographic separation. In contrast, a simple and rapid analytical method for trace detection of biochemical species is provided by study of electrodes modified with conducting polymer films, such as 3-methylthiophene, [16, 23, 24] hippuric acid, [25] and trans-3-(3-pyridyl) acrylic acid. [26] Major advantages of these

materials include highly-conductive surfaces, a large number of reactive sites, catalytic properties, pre-concentration ability, and surface- fouling prevention. Likewise, poly(3-acetylthiophene) (P3AT) is an important conducting polymer with excellent electrocatalytic effect on uric acid [27] and dopamine. Because adjusting electrochemical parameters can control film thickness, permeation and charge-transport characteristics, [28-30] electro-polymerization is a good approach to polymer immobilization, and readily deposits P3AT onto a given electrode's surface.

We have found no reports concerning the determination of 8-OH-dG on a P3AT-modified GCE. Here, we investigate the selective cytotoxicity of 3-MCPD on HEK293 cells by analyzing the cell growth inhibition, morphological changes, ROS production and DNA damage. By this means, we further demonstrate that 3-MCPD inhibits growth of cells and induces 8-OH-dG generation via ROS-mediated oxidative DNA damage in HEK293 cells. For electrochemical detection of 8-OH-dG in oxidation-damaged cells, we successfully prepared our P3AT-modified GCE through 3-AT electrodeposition on the electrode surface. P3AT conducting polymer exhibits dramatic electrocatalytic effect on the oxidation of 8-OH-dG and greatly enhances its peak current. We diminished interference due to presence of deoxyadenosine (dA) and deoxyguanosine (dG) sufficiently in 0.1 M pH 6.0 PBS. The created P3AT/GCE shows good sensitivity, high selectivity, excellent detection limit, and wide linear range. We successfully applied P3AT/GCE to determine levels of 8-OH-dG in real cell samples with satisfactory results, and the modified electrode proved both reproducible and stable.

2. Materials and methods

2.1. Reagents and chemicals

We purchased 3-MCPD, 8-Hydroxy-2'-deoxyguanosine, deoxyadenosine,

deoxyguanosine and acetonitrile from J&K Chemical. From Sigma (Aldrich, Spain), we obtained 3-acetylthiophene and $LiClO_4$. Sangon Biotech (Shanghai) Co., Ltd. provided 3-(4,5-dimethylthiazol-2-yl)-2,5-diphenyltetrazolium bromide (MTT), DNA extraction kit, deoxyribonuclease I (DNase I) and alkaline phosphatase (ALP). Reactive Oxygen Species Assay Kit was produced by Beyotime Institute of Biotechnology (Shanghai, China). Cell Biolabs Inc. (San Diego, CA) provided the OxiSelect™ Comet Assay Kit. Highly pure nitrogen was used for de-aeration. Other reagents were all analytical reagent grade, and all aqueous solutions were prepared with ultrapure water.

2.2. Cell culture and treatment

We obtained the HEK293 (human embryonic kidney) cell line from the cell bank at Chinese Academy of Sciences (Shanghai, China), which we then cultured in DMEM medium, supplemented with 10% heat-inactivated fetal bovine serum (FBS; Invitrogen) in a humidified 5% CO_2 incubator at 37℃. The serial dilution of 3-MCPD with serum-free culture media on cultured plates yielded final concentrations of 0.5, 1.0, 5.0, 10, 50, 100 mM. We applied untreated cells as controls in all experiments.

2.3. Analysis of 8-OH-dG by UPLC-MS/MS

In order to determine whether the HEK293cells stimulated by 3-MCPD produce 8-OH-dG, we used UPLC-MS/MS (Waters corporation, USA) for qualitative analysis of the typical biomarker for oxidative DNA damage. We prepared 8-OH-dG standard solution in methanol/water (1:1, v/v). Using 100 mM 3-MCPD for 24 h, we then stimulated 1.0×10^6 cells. After applying our DNA extraction kit, we hydrolyzed the product by enzymatic digestion with 5 U DNase I and 1 U ALP for 2h at 37℃ in a water bath. To remove the hydrolytic enzymes, we centrifuged the extract twice at 12000 rpm for 15 min, each. We vacuum-dried the supernatant and then dissolved this

in 100 μL methanol/water. The samples and 8-OH-dG standard solution were analyzed using UPLC-MS/MS.

Into a BEH300 C18 analytical column (100 mm × 2.1 mm i.d., 1.7 μm), we injected a 1-μL aliquot of the sample solution, and maintained the column at 30℃. The flow rate of the mobile phase was 300 μL/min. We executed a gradient elution (A [methanol] and B [0.1% formic acid in water]) on analytes from the column. The gradient was 5% A from 0-0.5 min., 5-100% A from 0.5-7 min., 100% A from 7-9 min., 100-5% A from 9-9.5 min.

For mass spectrum analysis, we employed the standard-flow ESI source and positive ion mode, setting dwell time to 106 ms and cone voltage at 18.0 V. We also employed optimal collision energies for all precursor/product MRM ion pairs (284.21/117.13, 284.21/140.15, and 284.21/168.13).

2.4. Fabrication of modified glassy carbon electrode

The CHI-760C electrochemical workstation (CH Inc., Shanghai, China) served as our platform for CV and DPV experiments. The conventional three-electrode system with a modified glass carbon electrode (GCE, φ 2 mm) served as the working electrode, a platinum wire as auxiliary electrode, and a saturated calomel electrode (SCE) served as reference.

We polished the bare GCE to a mirror finish using a slurry of alumina (0.30 and 0.05 μm), washing with ultrapure water, then ultrasonicating in ethanol and ultrapure water for 2 min. Before electrode modification, we activated the glassy carbon electrode in 0.1 M pH 6.0 phosphate buffer solution (PBS) from -1.6 - +2.0 V at a scan rate of 100 mV s^{-1} for 10 cycles (Fig. S1, Supporting Information), then rinsed with ultrapure water, and dried using N_2. Following reported methods [27] we prepared the P3AT-modified GCE. To summarize the process, we electrodeposited P3AT on a

GCE surface from a solution containing 10 mM 3-AT and 50 mM $LiClO_4$ as the supporting electrolyte, which we dissolved in acetonitrile by cyclic sweepings between -1.6 - +2.0 V at a scan rate of 50 mV s^{-1} for 20 scans. This induces the generation and polymerization of 3-AT free radicals on the GCE surface. After polymerization, we electroactivated the modified electrode by cyclic voltammetry from -0.2 - +0.7 V at 100 mV s^{-1} in pH 6.0 PBS, until we obtained a stable background. The final modified electrode is defined as P3AT/GCE.

2.5. Electrochemical experiments

We performed CV and DPV experiments in 0.1 M PBS containing either 35 or 70 μM 8-OH-dG. Under the various conditions, we recorded cyclic voltammograms (CVs) by scanning the potential range between -0.2 - +0.7 V at a scan rate of 100 mV s^{-1}. We executed the differential pulse voltammograms (DPVs) over an applied potential range from −0.2 - +0.6 V with the DPV parameters as follows: pulse amplitude of 100 mV, sample width of 16.7 ms, pulse width of 60 ms, 200 ms pulse period and a 2 s quiet time. All experiments proceeded at ambient temperature.

2.6. Detection of 8-OH-dG in real cell samples

We stimulated 1.0×10^7 HEK293 cells by 1, 10, 50, and 100 mM 3-MCPD for 24 h. We kit-extracted DNA from the cells and characterized the extract by agarose gel electrophoresis (Fig. S2, Supporting Information), according to the method we describe in Section 2.4. Using 1 mL of 0.1 M pH 6.0 PBS, we then dissolved the supernatant. The samples were spiked with 8-OH-dG standard solution and analyzed by the proposed method.

2.7. Statistical analysis

Using a one-way analysis of variance (ANOVA) test, we determined statistical significance. *Post hoc* comparisons (LSD) served to discriminate

differences between mean values. We express results as means ± SD. A value of $P < 0.05$ indicates statistical significance.

3. Results and discussion

3.1. Assessment of oxidative damage in 3-MCPD-treated HEK293 cells

MTT assayed the number of viable cells. Treatment with 3-MCPD (0.5, 1.0, 5, 10, 50 and 100 mM) results in a dose-dependent suppression of cell viability (Fig. S3A). Significant decrease in treated-group cell viability (1, 10, 50 and 100 mM) in comparison to the control was revealed by *post hoc* analysis. To examine whether 3-MCPD exposure induces morphological changes in HEK293 cells, we incubated cells with 3-MCPD for 24 h, then examined them by LSCM. We observed both a decrease in the total cell number and an increase in floating cells (data not shown), with cell shrinkage and cytoplasm vacuolization in 3-MCPD-treated HEK293 cells. Meanwhile, control HEK293 cells were intact in shape (Fig. S3B). These results show that 3-MCPD-induced morphological changes took place in HEK293 cells. Using DCFH-DA, we observed ROS level in HEK293 cells to evaluate its direct effect on 3-MCPD-induced oxidation stress. We harvested cells to evaluate ROS level after incubation with 3-MCPD (1.0-100 mM) for 24 h. A marked increase in ROS level appeared following 100 mM 3-MCPD treatment, approximately three-fold that of unexposed control cells (Fig. S3C and D). This phenomenon indicates ROS formation is involved in 3-MCPD-induced apoptosis in HEK293 cells. By applying the neutral version of the Comet assay to determine strand breaks and a few AP sites, we measured DNA damage in HEK293 cells treated with 3-MCPD (Fig. S3E). In the comet assay, damaged DNA fragments migrate out of the cell nucleus as a streak similar to the tail of a comet, and the quantified olive tail moment (OTM) is directly proportional to the amount of DNA damage. The mean OTM value of the negative

control is 0.17 ± 0.071 (SD). Rising 3-MCPD concentration signals an increase in DNA damage (Fig. S1F). Moreover, cells treated with 50 mM and 100 mM 3-MCPD show significantly greater OTM. Our results indicate that 3-MCPD induces oxidative DNA damage in HEK293 cells.

3.2. Analysis of 8-OH-dG by UPLC-MS/MS

We used UPLC-MS/MS to qualitatively analyze 8-OH-dG in 3-MCPD-stimulated HEK293 cells. As shown in Figure S4, the major peak retention time of the test solution corresponds to that of the standard 8-OH-dG solution. This correspondence indicates that the 3-MCPD-treated HEK293cells produced 8-OH-dG. Therefore, we can detect the oxidative DNA damage in hazardous substance exposure to cells by the electrochemical method, based on redox activity of 8-OH-dG.

3.3. Fabrication and characterization of the P3AT modified electrode

We prepared the P3AT/GCE by electropolymerization using cyclic voltammetry. Figure 1 portrays typical glassy carbon electrode CVs obtained by scanning electropolymerization from -1.6 - +2.0 V in a fresh acetonitrile solution of 3-AT and $LiClO_4$. In the first cyclic scan, two anodic peaks (1 and 2) and one cathodic peak (3) occur near the respective potential values of 0.45 V, 1.19 V, and -0.9 V. Oxidation peak potentials gravitate slightly to the negative, and the reduction peak potential shifts positively upon continuous scanning, perhaps indicating that the polymer redox occurs more readily than the monomer. [31] With increasing scan cycles, redox peak currents also gradually increase. Over the first five cycles, peak currents increase more quickly than the other cycles, reaching a steady state after the eighth cycle. This demonstrates that further cyclic scanning in the applied potential window produces little growth on the conducting polymer film. Results indicate that a uniform adherent P3AT polymer film successfully deposited on the GCE surface via

electropolymerization.

We used a ferrocyanate $[Fe(CN)_6]^{3-/4-}$ redox couple as an electrochemical probe to investigate the electrochemical activity of the P3AT-modified GCE. As shown in Fig. S5A, the bare GCE exhibits a couple of redox peaks with a peak potential separation (ΔE_P) of 98 mV and an I_P ratio of about 1:1 in curve a. As shown in curve b, a decrease in the ΔE_P (70 mV) and an increase in the I_P were obtained once we modified the GCE with P3AT. We attribute this to an increase in electrocatalytic effect and the effective surface area of the P3AT, in turn greatly increasing the electron transfer rate of $[Fe(CN)_6]^{3-/4}$. At the same time, $[Fe(CN)_6]^{3-/4-}$ anodic and cathodic peak currents are linearly related to square root of scan rate at the P3AT/GCE. As shown in Fig. S5B, their regression equations are: $I_{pa} = -2.3806\nu^{1/2} - 3.8875$ (R^2 = 0.9937) and $I_{pc} = 2.6009\nu^{1/2} + 3.2908$ (R^2 = 0.9955) (I_p: μA, ν: mV s^{-1}). The inset plot indicates considerable improvement of electron transfer on $[Fe(CN)_6]^{3-/4-}$ by the conducting P3AT polymer with a diffusion-controlled process on P3AT/GCE.

3.4. Electrochemical behaviors of 8-OH-dG on P3AT modified electrode

Fig. 2 shows the CVs (A) and DPVs (B) for 35 μM 8-OH-dG in 0.1 M PH 6.0 PBS at the bare GCE (a) and P3AT/GCE (b). We observed an irreversible oxidation process at both electrodes. The anodic peak current signal of 8-OH-dG is significantly enhanced compared with the electrochemical response on bare electrode. Oxidative potential changed negatively in the case of P3AT/GCE, perhaps due to improvement in electron transfer properties and the large surface area of P3AT.

The presence of 8-OH-dG and/or its oxidation products is usually believed to foul the bare electrodes by accumulation. [32] Therefore, after repeated cycle scans, the inhibitory layer formed on the bare electrode results in a decrease in the anodic peak current (Fig. 2C). In contrast, we observed unchanged wave shape and lack of

degraded response for the entire series at the P3AT electrode, exhibiting a good resistance to fouling in the presence of high concentrations of 8-OH-dG (Fig. 2D). We attribute such a high state of surface cleanliness to the use of the novel P3AT conducting polymer substrate on which oxidation products do not deposit. The high stability implies that repetitive surface renewal schemes are no longer necessary where 8-OH-dG voltammetry is concerned.

3.5. Optimization of the electrochemical sensor

The pre-concentration potential and time are critical factors influencing the modified electrode sensitivity in DPV technique. Fig. 3 shows variation of 8-OHdG oxidation currents obtained as a function of pre-concentration potential and time. We incubated the P3AT/GCE over different potentials in the range of -600-150 mV to determine the optimum pre-concentration potential for the detection of 8-OH-dG. The highest current was observed when the pre-concentration potential was -350 mV (Fig. 3A). As shown in Fig. 3B, the anodic peak current gradually increased and reached maximum at about 7.0 min., remaining stable over 8 min., translating to saturation at about 7.0 min of available sites on P3AT/GCE surface. Thus we found, for the ensuing sections, the best compromise between the sensitivity and the time required for the analysis: a pre-concentration potential of -350 mV and a pre-concentration time of 7.0 min.

The effect of supporting electrolyte pH on current response and oxidation potential of 8-OH-dG on P3AT/GCE were investigated by the DPV mode. As shown in Fig. 4A, electrochemical behavior of 8-OH-dG on P3AT/GCE is considerably influenced by the pH value of the supporting electrolyte. With increasing pH in the range of 4-10, the oxidation peak potential of 8-OH-dG shifts negatively, indicating a proton-transfer process is involved in the electrochemical reaction of 8-OH-dG. [33] The

oxidation peak potential has a linear correlation with the pH of the supporting electrolyte between 4-10 (Fig. 4B). Here, the linear regression equation is $E_{pa} = -0.0641pH + 0.7159$ with a correlation coefficient of 0.9993. The slope of 64.1 mV/pH implies that the number of electrons and protons in the process are equal, which is consistent with previous results. [32] The number of hydrogen ions involved in the whole electrode reaction is 2. [12] The interception has a 755.9 mV value, which represents the standard potential of the reaction under the experimental conditions. Furthermore, the 8-OH-dG anodic peak current increases gradually along with pH to about 6.0, and then decreases with further pH increase (Fig. 4B). Therefore, we chose 0.1 M pH 6.0 PBS for the electrochemical detection of 8-OH-dG in the following sections.

Fig. 4C and D illustrate the scan rate impact on the electrochemical response of 35 μM 8-OH-dG on P3AT/GCE using cyclic voltammetry in 0.1 M PBS at pH 6.0. We observed that the anodic peak current increases and the peak potential gradually shifts positively with increased scan rates (Fig. 4C). The oxidation current is linear with the square root of the scan rate over the range of 5-300 mV s^{-1} (Fig. 4D). In this case, the linear regression equation is $I_{pa} = 0.0594\nu^{1/2} - 0.033$ (I_{pa} in μA and ν in mV s^{-1}) with a correlation coefficient of 0.9943, suggesting that 8-OH-dG undergoes a diffusion-controlled process on the surface of the P3AT-modified electrode.

3.6. Electrochemical detection of 8-OH-dG at P3AT/GCE

Applying DPV technique in 0.1 M de-aerated PBS of pH 6.0, we determined the 8-OH-dG concentration, for which we required a pre-concentration time of 7.0 min. at -350 mV constant potential. After every measurement, we cleaned the modified electrode by cyclic voltammetry in pH 6.0 PBS to eliminate 8-OH-dG adsorption, thus renewing the electrode surface. We plotted the anodic peak currents against the

bulk concentration of 8-OH-dG from 0.5-60 μM (Fig. 5). Here, we see that increase in DPV signals is directly related to increase in 8-OH-dG concentration (Fig. 5A). A linear behavior between the DPV current and the 8-OH-dG concentration occurs from 0.5-35μM (Fig. 5B). Here, the linear regression equation is $I_{pa} = 0.123C - 0.0163$ (I_{pa} in μA and C in μM) with a correlation coefficient of 0.9963. The detection limit and the quantification limit are 31.3 nM (S/N=3) and 104 nM (S/N=10), respectively. Other authors using techniques such as HPLC-ECD [34] obtained data comparable to ours.

3.7. Interference study

Because they are major electroactive molecules and have very similar structures to that of 8-OH-dG, it is accepted that dA and dG coexist with 8-OH-dG in the oxidation-damaged DNA and may interfere with 8-OH-dG electrochemical signal in real sample detection. We therefore performed the interference study by determining the DPV response of 8-OH-dG in the presence of dA and dG. As shown in Fig. 6, the presence of about 20-fold excess of dA and dG relative to 8-OH-dG does not interfere with the response of 8-OH-dG at 0.32 V. As well, the anodic peaks of 8-OH-dG, dG and dA divide completely into three voltammetric peaks at potentials of around 0.32 V, 0.64 V and 0.95 V, respectively. Separation of oxidation peak potentials for 8-OH-dG and dG, 8-OH-dG and dA are about 320 mV and 630 mV, respectively. The two-peak potential differences are large enough to avoid the interference of dA and dG on 8-OH-dG in a homogeneous solution. P3AT/GCE possesses good preferential adsorption and catalytic activity for the electrochemical oxidation of 8-OH-dG, according to our results.

3.8. The reproducibility and stability of the P3AT/GCE

To evaluate the reproducibility and repeatability of our P3AT/GCE, we carried out experiments in 35 μM 8-OH-dG in 0.1 M pH 6.0 PBS. Using five different GCE electrodes, we regenerated the P3AT/GCE with a peak current RSD of 2.8 %. We also found that the anodic peak height remains nearly the same with a relative standard deviation of 2.13% for 10 determinations, indicating good reproducibility. After the measurement, we cleaned the modified electrode with voltammetric cycles, storing it in pH 6.0 PBS at 4℃, and re-measuring at intervals of several days. The peak current decreased about 10% in 1week, and decreased to 76 % of the initial current after two weeks. All measurements indicate that P3AT/GCE possesses excellent stability.

3.9. Application in real cell samples

We tested the possibility of using P3AT/GCE for the determination of 8-OH-dG in practical cell samples. After extracting DNA from the normal HEK293 cells and enzymolysizing, we spiked the samples with 10, 20, and 30 μM 8-OH-dG in 0.1 M pH 6.0 PBS, respectively. Employing the established method for the three different determinations, we obtained satisfactory average recoveries of 101.4 %, 97.5 %, and 98.3 % with relative standard deviations of 2.61 %, 2.92 %, and 2.47 %.

We further applied the P3AT/GCE to detect 8-OH-dG level in HEK293 cells treated with varied concentrations of 3-MCPD for 24 h. The 8-OH-dG level increased from 195 to 633 nM with increased 3-MCPD concentration from 0-100 mM (Fig. 7). This is consistent with rising of ROS levels, indicating the oxidative DNA damage in HEK293 cells is probably induced by the increased level of intracellular ROS and formation of 8-OH-dG. As indicated by our results, the proposed modified electrode is suitable for estimation of 8-OH-dG level in cells suffering from oxidative DNA damage.

4. Conclusions

In conclusion, we have shown that 3-MCPD has cytotoxic effects on HEK293 cells and this effect occurs largely via intracellular ROS increase, which is linked to ability of ROS to trigger oxidative DNA damage in cells. We also found that electro-polymerization is an effective fabrication method for poly(3-acetylthiophene)-modified glassy carbon electrode as applied to electrochemical detection of 8-OH-dG. The modified electrode exhibits high electrocatalytic activity towards the oxidation of 8-OH-dG, greatly accelerating its electron transfer rate. In 0.1 M pH 6.0 PBS, the anodic peak currents of DPVs are linear with 8-OH-dG concentration from 0.5-35 μM, with a detection limit of 31.3 nM. The P3AT/GCE presents favorable selectivity for 8-OH-dG detection free of interference of excess dA and dG, also showing excellent reproducibility and stability. We also utilized the proposed method with satisfactory results for the determination of 8-OH-dG in real cell samples.

Acknowledgements

This work was supported by the "973" National Basic Research Program of China (No. 2012CB720804), the National Research Program (No. 201003008-08, No. 201203069-1), the Program for New Century Excellent Talents in Jiangnan University, Qinglan project，Synergetic Innovation Center Of Food Safety and Quality control, and Priority Academic Program Development of Jiangsu Higher Education Institutions, and the Priority Academic Program Development of Jiangsu Higher Education Institutions.

References

1. P. J. Nyman, G. W. Diachenko and G. A. Perfetti, *Food Additives & Contaminants*, 2003, 20, 909-915.
2. L. Liu, Y. He, H. Lu, M. Wang, C. Sun, L. Na and Y. Li, *Journal of Chromatography B*, 2013, 927, 97-104.
3. J. B. Cavanagh and C. C. Nolan, *Neuropathology and Applied Neurobiology*,

1993, 19, 471-479.

4. J. Velisek, J. Davidek, V. Kubelka, G. Janicek, Z. Svobodova and Z. Simicova, *Journal of Agricultural and Food Chemistry*, 1980, 28, 1142-1144.

5. R. El Ramy, M. Ould Elhkim, S. Lezmi and J. M. Poul, *Food and Chemical Toxicology*, 2007, 45, 41-48.

6. J. K. Lee, J. A. Byun, S. H. Park, H. S. Kim, J. H. Park, J. H. Eom and H. Y. Oh, *Toxicology*, 2004, 204, 1-11.

7. H. Kasai, *Mutation Research/Reviews in Mutation Research*, 1997, 387, 147-163.

8. A. Pilger and H. W. Rüdiger, *International Archives of Occupational & Environmental Health*, 2006, 80, 1-15.

9. L. Chi-Shan, W. Kuen-Yuh, C.-C. Gou-Ping and C. Chin-Cheng, *Environmental Science & Technology*, 2005, 39, 2455-2460.

10. M. K. Shigenaga and B. N. Ames, *Free Radical Biology and Medicine*, 1991, 10, 211-216.

11. R. A. Floyd, J. J. Watson, P. K. Wong, D. H. Altmiller and R. C. Rickard, *Free radical research communications*, 1986, 1, 163-172.

12. A. Gutiérrez, S. Gutiérrez, G. García, L. Galicia and G. A. Rivas, *Electroanalysis*, 2011, 23, 1221-1228.

13. A. Gutierrez, S. Osegueda, S. Gutierrez-Granados, A. Alatorre, M. G. Garcia and L. A. Godinez, *Electroanalysis*, 2008, 20, 2294-2300.

14. K. Tamae, K. Kawai, S. Yamasaki, K. Kawanami, M. Ikeda, K. Takahashi, T. Miyamoto, N. Kato and H. Kasai, *Cancer Science*, 2009, 100, 715-721.

15. C. Matayatsuk and P. Wilairat, *Journal of Analytical Chemistry*, 2008, 63, 52-56.

16. T. H. Li, W. L. Jia, H. S. Wang and R. M. Liu, *Biosensors & Bioelectronics*, 2007, 22, 1245-1250.

17. S. W. Zhang, C. J. Zou, N. Luo, Q. F. Weng, L. S. Cai, C. Y. Wu and J. Xing, *Chin. Chem. Lett.*, 2010, 21, 85-88.

18. S. D. Arnett, D. M. Osbourn, K. D. Moore, S. S. Vandaveer and C. E. Lunte, *J. Chromatogr. B*, 2005, 827, 16-25.

19. S. R. Mei, Q. H. Yao, C. Y. Wu and G. W. Xu, *J. Chromatogr. B*, 2005, 827, 83-87.

20. B. Crow, M. Bishop, K. Kovalcik, D. Norton, J. George and J. A. Bralley, *Biomed. Chromatogr.*, 2008, 22, 394-401.

21. J. L. Ravanat, P. Guicherd, Z. Tuce and J. Cadet, *Chem. Res. Toxicol.*, 1999, 12,

802-808.

22. Y. Y. Han, M. Donovan and F. C. Sung, *Chemosphere*, 2010, 79, 942-948.

23. X. Huang, Y. Li, P. Wang and L. Wang, *Analytical Sciences*, 2008, 24, 1563-1568.

24. J. Wang and R. Li, *Analytical Chemistry*, 1989, 61, 2809-2811.

25. H. Zhao, Y. Zhang and Z. Yuan, *Electroanalysis*, 2002, 14, 1031-1034.

26. Y. Zhang, S. Su, Y. Pan, L. Zhang and Y. Cai, *Annali di Chimica*, 2007, 97, 665-674.

27. M. Aslanoglu, A. Kutluay, S. Abbasoglu and S. Karabulut, *Chemical and Pharmaceutical Bulletin*, 2008, 56, 282-286.

28. G. Milczarek and A. Ciszewski, *Electroanalysis*, 2003, 15, 529-532.

29. H. R. Zare, N. Nasirizadeh and M. Mazloum Ardakani, *Journal of Electroanalytical Chemistry*, 2005, 577, 25-33.

30. P. R. Roy, T. Okajima and T. Ohsaka, *Bioelectrochemistry*, 2003, 59, 11-19.

31. Y. Pang, X. Li, H. Ding, G. Shi and L. Jin, *Electrochimica Acta*, 2007, 52, 6172-6177.

32. J. Langmaier, Z. Samec and E. Samcová, *Electroanalysis*, 2003, 15, 1555-1560.

33. T.-H. Li, W.-L. Jia, H.-S. Wang and R.-M. Liu, *Biosensors and Bioelectronics*, 2007, 22, 1245-1250.

34. T. Hofer and L. Moller, *Chem. Res. Toxicol.*, 1998, 11, 882-887.

Figure Captions

Fig.1. CVs of 10 mM 3-AT in acetonitrile containing 50 mM $LiClO_4$. Scan rate: 50 mV s^{-1}, scan cycles: 10.

Fig.2. (A) CVs and (B) DPVs for 35 μM 8-OH-dG in 0.1 M PH 6.0 PBS at the bare GCE (a) and P3AT/GCE (b). Successive CVs (a-e) for 35 μM 8-OH-dG at the bare GCE (C) and P3AT/GCE (D).

Fig.3. (A) DPV responses of 35 μM 8-OH-dG at different pre-concentration potentials from -600 to 150 mV. (B) DPV responses of 70 μM 8-OH-dG at different pre-concentration times from 0.5 to 15 min. All of them were obtained on P3AT/GCE. Supporting electrolyte: 0.1 M PH 6.0 PBS.

Fig.4. (A) DPVs of 70 μM 8-OH-dG in 0.1M PBS with different pH values at the P3AT/GCE. (B) E_{pa} and I_{pa} vs. pH plot. (C) CVs of 35 μM 8-OH-dG in 0.1 M PH 6.0 PBS on P3AT/GCE at different scan rate: 5, 10, 20, 40, 60, 80, 100, 150, 200 and 300 mV s^{-1}. (D) Calibration plots of the anodic peak current versus the square root of scan rate on P3AT/GCE.

Fig.5. (A) DPVs for different concentrations of 8-OH-dG: (a-j) 0.5, 1, 5, 10, 15, 20, 25, 35, 50 and 60 μM. (B) Calibration plots for 8-OH-dG.

Fig.6. DPVs of 5 μM 8-OH-dG in the absence (a) and presence (b) of 100 μM dG and 100 μM dA at the P3AT/GCE. Inset: DPVs of 100 μM dG and 100 μM dA at the GCE, respectively.

Fig.7. DPV responses of 8-OH-dG in HEK 293 cells treated with different concentrations of 3-MCPD for 48 h.

Fig.1

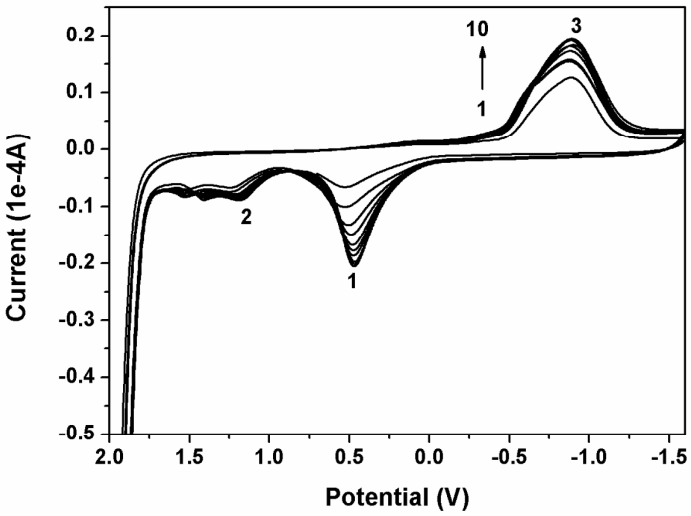

Fig.2

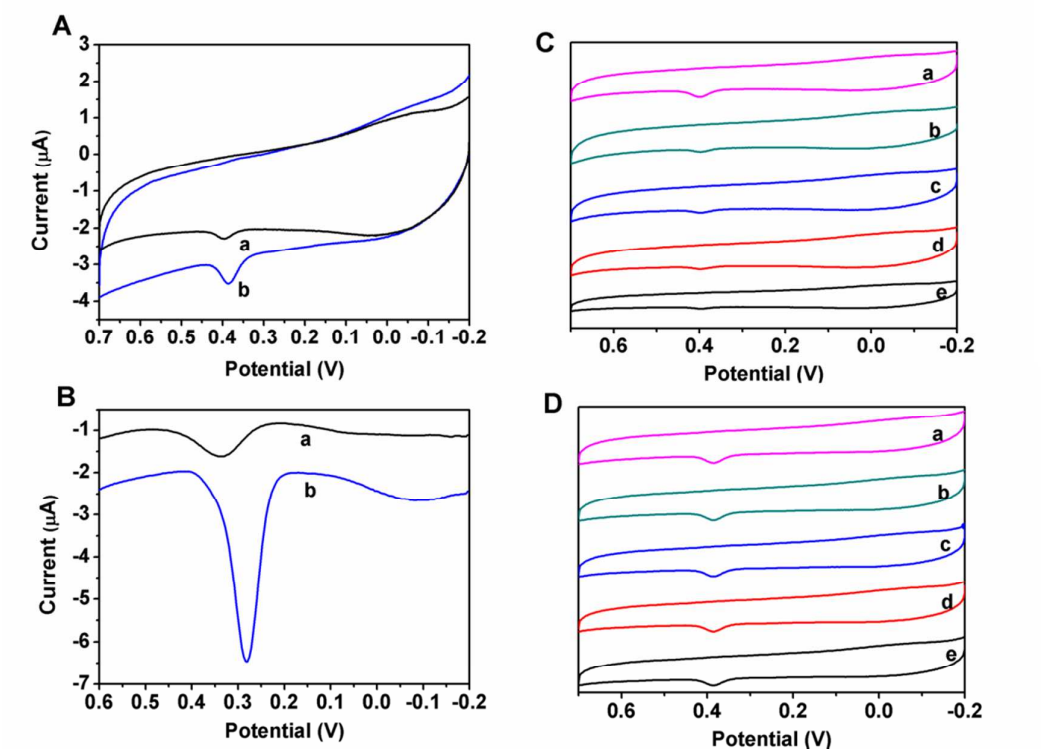

Fig.3

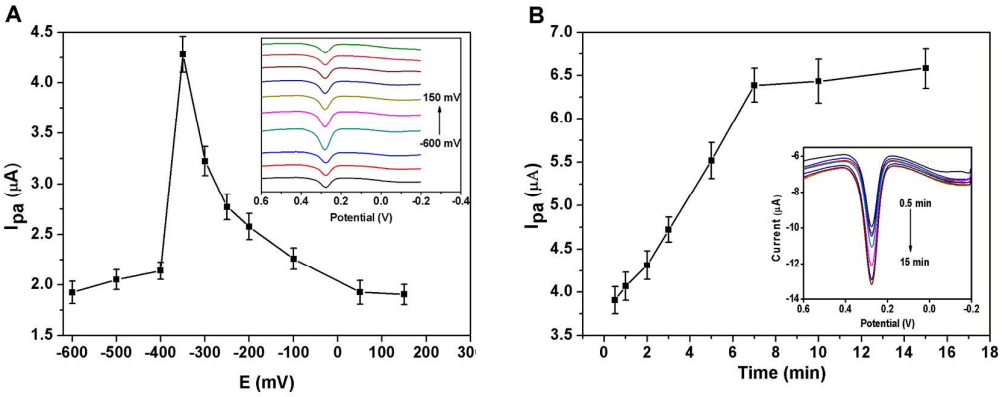

Fig.4

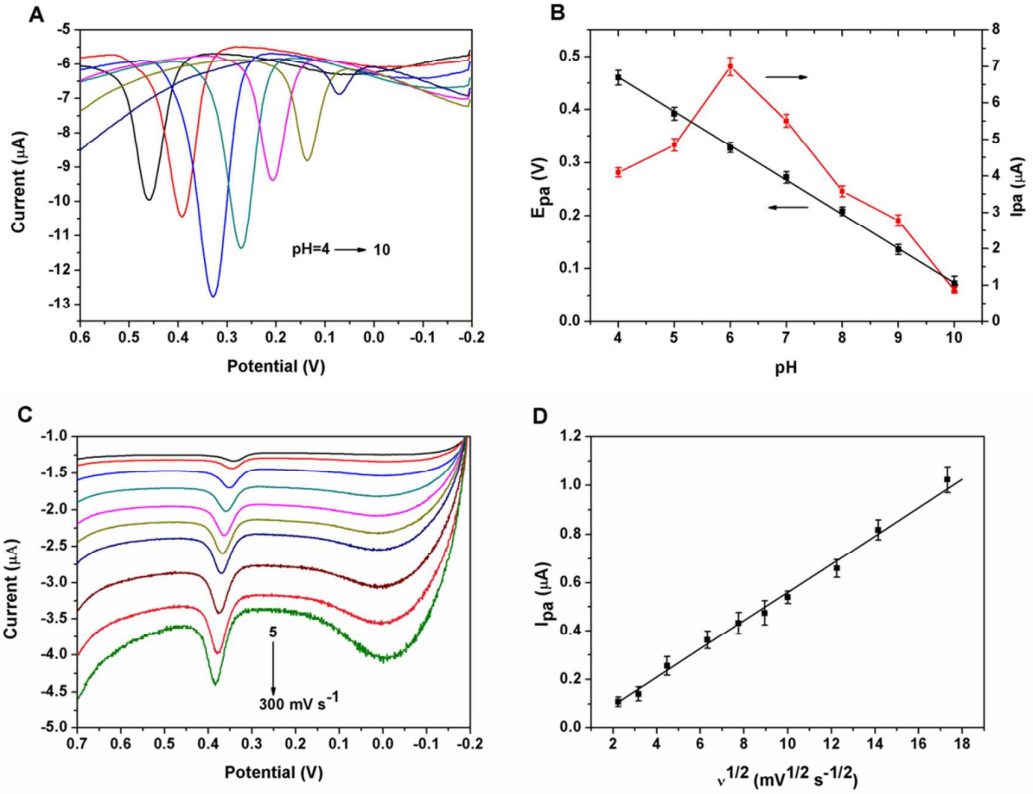

Fig.5

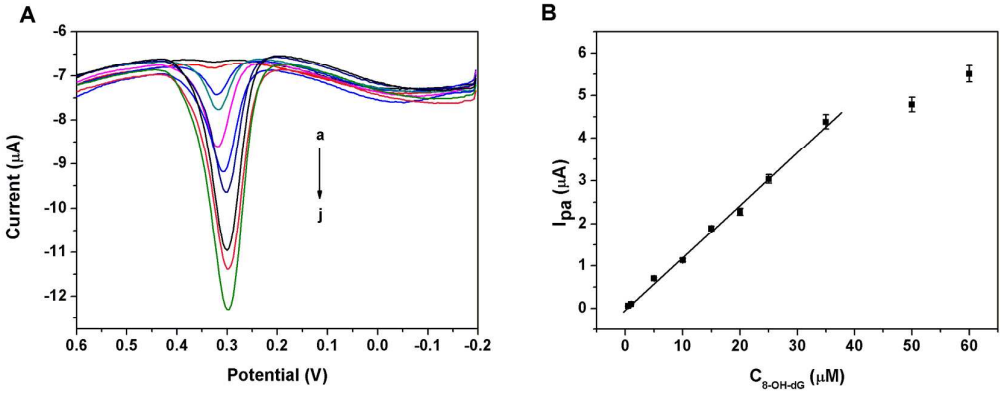

Fig.6

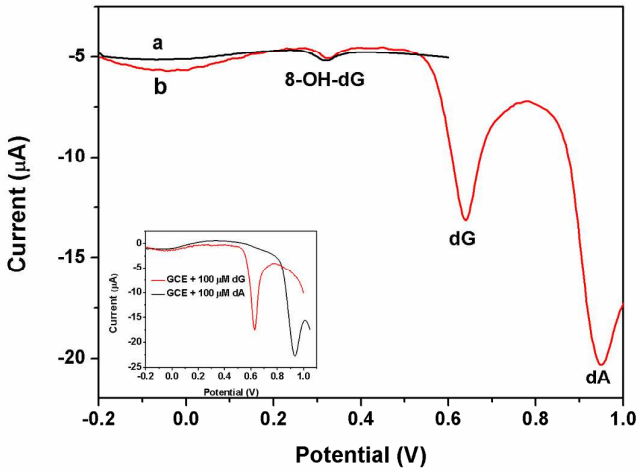

Fig.7

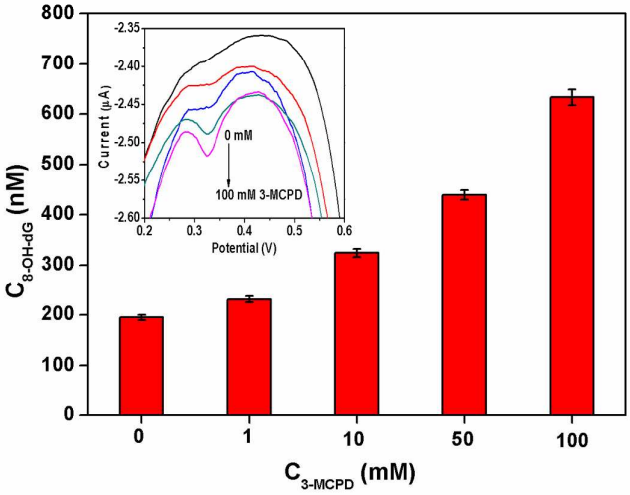

schematic diagram

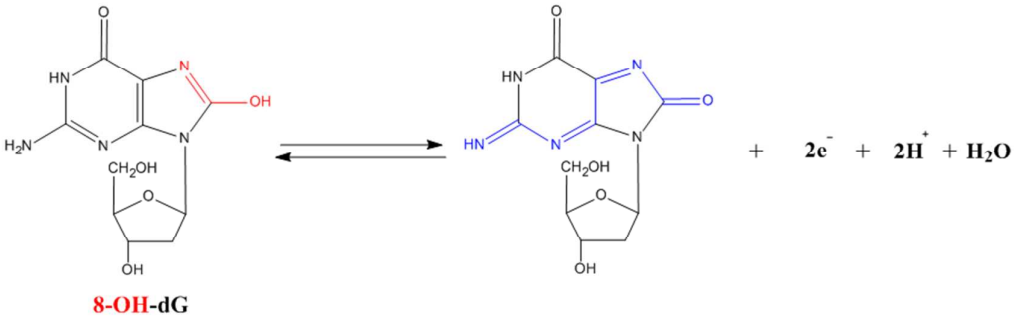

8-OH-dG